Available online at www.sciencedirect.com

ScienceDirect

Chronic Diseases and Translational Medicine 2 (2016) 181−188

www.keaipublishing.com/en/journals/cdtm/

www.cdatm.org

Original Article

Intraoperative high-field magnetic resonance imaging, multimodal neuronavigation, and intraoperative electrophysiological monitoring-guided surgery for treating supratentorial cavernomas

Fang-ye Li, Xiao-lei Chen*, Bai-nan Xu

Department of Neurosurgery, Chinese People's Liberation Army General Hospital, Beijing 100853, China

Received 27 October 2016

Available online 7 December 2016

Abstract

Objective: To determine the beneficial effects of intraoperative high-field magnetic resonance imaging (MRI), multimodal neuronavigation, and intraoperative electrophysiological monitoring-guided surgery for treating supratentorial cavernomas.

Methods: Twelve patients with 13 supratentorial cavernomas were prospectively enrolled and operated while using a 1.5 T intraoperative MRI, multimodal neuronavigation, and intraoperative electrophysiological monitoring. All cavernomas were deeply located in subcortical areas or involved critical areas. Intraoperative high-field MRIs were obtained for the intraoperative "visualization" of surrounding eloquent structures, "brain shift" corrections, and navigational plan updates.

Results: All cavernomas were successfully resected with guidance from intraoperative MRI, multimodal neuronavigation, and intraoperative electrophysiological monitoring. In 5 cases with supratentorial cavernomas, intraoperative "brain shift" severely deterred locating of the lesions; however, intraoperative MRI facilitated precise locating of these lesions. During long-term (>3 months) follow-up, some or all presenting signs and symptoms improved or resolved in 4 cases, but were unchanged in 7 patients.

Conclusions: Intraoperative high-field MRI, multimodal neuronavigation, and intraoperative electrophysiological monitoring are helpful in surgeries for the treatment of small deeply seated subcortical cavernomas.

Keywords: Cavernoma; Intraoperative electrophysiological monitoring; Intraoperative magnetic resonance imaging; Multimodal neuronavigation

Introduction

Since the advent of the intraoperative MRI system in the 1990s, it has been commonly accepted that the primary indication for intraoperative MRI and functional neuronavigation is the presence of neoplastic lesions, such as gliomas and pituitary adenomas.[1−9] Intraoperative MRI is used to find tumor remnants, to compensate for "brain shift," and to update the functional neuronavigation. However, the number of

* Corresponding author.
E-mail address: neurogz@foxmail.com (X.-l. Chen).

Peer review under responsibility of Chinese Medical Association.

Production and Hosting by Elsevier on behalf of KeAi

http://dx.doi.org/10.1016/j.cdtm.2016.11.003

studies regarding the clinical application of intraoperative MRI and multimodal neuronavigation for the treatment of supratentorial cavernomas is limited.[10−12]

As "benign" lesions, supratentorial cavernomas have relatively clear margins within the surrounding brain parenchyma. The goal of surgery for a cavernoma is the complete resection of the nidus and the surrounding epileptic foci.[13] If the nidus or epileptic foci involve eloquent structures (distance < 1 cm), complete resection may cause postoperative neurological deficits. In addition, precisely locating small deeply seated cavernomas is difficult when using conventional neuronavigation.

We sought to evaluate the clinical feasibility and accuracy of intraoperative high-field MRI and multimodal neuronavigation in the surgical treatment of supratentorial cavernomas.

Methods

Between February 2010 and October 2011, twelve right-handed patients with supratentorial cavernomas were prospectively enrolled in our study. All patients underwent intraoperative high-field MRI and multimodal neuronavigation-guided surgical treatment. Of the 12 patients, 6 were male and 6 were female. The mean age of the patients in this series was 36.3 years (standard deviation = 19.0 years, range: 10−61 years).

Conventional anatomical MRI (T1-weighted, T2-weighted, T2 fluid-attenuated inversion-recovery, post-contrast T1-weighted), diffusion tensor imaging (DTI), functional magnetic resonance imaging (fMRI), magnetic resonance angiography (MRA), magnetic resonance venogram (MRV), and diffusion weighted imaging (DWI) data were prospectively collected. All patients underwent preoperative, intraoperative, and postoperative MRI scans and preoperative and postoperative functional evaluation (motor, language, and vision). The local ethical committee approved the use of intraoperative high-field MRI. Signed informed consent was provided by the patient or by the appropriate family members.

Preoperative and intraoperative image acquisition

Preoperative and intraoperative MRI were performed using a 1.5-Tesla MAGNETOM Espree scanner (Siemens, Erlangen, Germany) using the same imaging protocol. The details of the pre- and intraoperative MRI sequences and paradigms have been previously published.[14,15] Imaging sequences were applied in the same transverse plane. All patients were positioned in the bore with the head centered in a standard eight-channel head coil. Intraoperative MRI scans were performed immediately after the operator believed that the lesion was totally removed or when necessary to correct for intraoperative brain shifts.

For DTI, we used a single-shot spin-echo diffusion weighted echo planar imaging (EPI) sequence (echo time of 147 ms, repetition time of 9400 ms, field of view of 250 × 250 mm^2, slice thickness of 3 mm, bandwidth of 1502 Hz/Px, diffusion encoding gradients in 12 directions, b values of 0 and 1000 s/mm^2, 40 slices, no intersection gap, and repeated 5 times).

Blood oxygen level dependent functional magnetic resonance imaging (BOLD-fMRI) was performed using a block design paradigm composed of task and rest periods to locate the eloquent cortex. To locate the language and visual cortices, subvocal counting, picture naming, or verb generation was performed by the patient to activate Broca's and Wernicke's areas. A standard 8-Hz checkerboard was used to find the visual cortex. To locate the motor cortex, alternate finger tapping (hand), up and down movement in the upper ankle joint (foot), or lip movements were used to activate the corresponding motor cortices.

MRI dataset processing

All preoperative, intraoperative, and postoperative MRI dataset analyses were processed using the dedicated navigation planning software iPlan 3.0 (Brainlab, Feldkirchen, Germany). Different sets of images were fused so that the MRI datasets could be processed as co-registered high-resolution three-dimensional (3D) anatomical images. Lesion segmentation, fiber tracking, and eloquent cortex localization were performed by the first author, who was blinded to the results of the neurological evaluations.

The minimum distance between the eloquent structures and the lesions was measured. Upon completion of the preoperative surgical plan, all integrated functional datasets and conventional anatomical images were transferred into the standard intraoperative multimodal neuronavigation system. Preoperatively, integrated functional data, including fMRI data, fiber tract data, data regarding the segmentation of the lesions, and anatomical images were used to delineate the 3D spatial relationships between brain structures and the lesions. An optimal surgical trajectory to access the lesions was decided on the basis of the preoperative 3D images of the lesion and the surrounding eloquent structures.

Intraoperative microscope-based multimodal neuronavigation

Intraoperative microscope-based multimodal neuronavigation was facilitated by a ceiling mounted VectorVision Sky navigation system (BrainLab, Feldkirchen, Germany). A conventional operating microscope (Pentero, Carl-Zeiss, Oberkochen, Germany) was connected to the functional neuronavigation system after the registration of previously collected 3D datasets. Integration of the functional datasets and other anatomical images into the 3D MPRAGE dataset enable the visualization of the contours of the lesions and nearby eloquent structures in the surgical field within the microscope ocular. This allows the surgeon to have an intuitive 3D impression of the location of the eloquent structures *in situ* so that he or she is able to remove the maximum amount of the lesion without increasing morbidity.[16] Additionally, co-registration of the microscope simplified the surgical procedures, as the neurosurgeons who performed the surgeries looked through the microscope instead of at a navigation screen. The contours of the lesions and eloquent structures were projected and drawn onto the scalp, reducing the size of the craniotomy and increasing the accuracy of the lesion localization.

Intraoperative MRI was implemented to compensate for brain shift and to evaluate the extent of the resection of the lesions. If the intraoperative images depicted residual lesions that could be further removed, intraoperative MRI datasets, including anatomical and functional images, were used to update the neuronavigation system.

Clinical evaluation

All patients had clinical neurological evaluations both preoperatively and postoperatively. The evaluations were performed by experienced specialists who were blinded to the results of the neuroimaging findings.

The Chinese Western Aphasia Battery (WAB), which consists of spontaneous speech, auditory verbal comprehension, repetition, and naming, was used to assess language deficits.[17] The patients had preoperative and postoperative visual field examinations by experienced ophthalmologists blinded to the neuroimaging findings. The evaluations were carried out using a Humphrey Field Analyzer II (Carl Zeiss, Meditec, Japan). Muscle strength was graded on the basis of the Royal Medical Research Council of Great Britain (MRC) scale.[18,19] Cavernous malformations were classified according to the Zabramski classification.[20−22]

Surgical strategies and intraoperative electrophysiological monitoring

The primary goal of surgical treatment for cavernous malformations is gross total resection of lesions and epileptic foci (if possible), while preserving nearby eloquent structures. Direct cortical stimulation using a bipolar stimulator was performed for lesions close to the motor cortex. Corresponding motor evoked potentials (MEPs) were recorded to identify the motor cortex intraoperatively. Intraoperative electrophysiological monitoring was used to identify epileptogenic areas in patients presenting with epilepsy.

Statistics

Statistical analyses were performed using the Statistical Package for the Social Sciences software (version 14.0; SPSS, Inc., Chicago, IL). Fisher's Exact Test was used to compare the preoperative estimation of brain shift to the intraoperative findings. P values <0.05 were considered statistically significant.

Results

Conventional MRI evaluation

All cavernomas were deeply seated in subcortical areas or involved eloquent structures. There were 2 type I, 3 type II, and 8 type III lesions in the 12 patients with supratentorial cavernomas. No type IV lesions were found. An overview of the measured data is depicted in Table 1.

Intraoperative surgical treatment

Eloquent cortices, such as Broca's, Wernicke's, hand, foot, lip, and visual cortices, were successfully activated and depicted. Critical fiber tracts, including the corticospinal tracts, medial lemniscuses, the arcuate fasciculus, and the optic radiation, were also successfully generated in appropriate cases. 3D relationships between lesions and integrated eloquent data suggested suitable and safe surgical intraoperative trajectories to the lesions.

In 5 (41.7%) of the 12 patients with supratentorial cavernomas, intraoperative brain shifts severely interfered with determination of the locations of the lesions. However, the surgeons had preoperatively estimated an obvious brain shift in 2 cases ($P = 0.37$). Intraoperative MRI helped to update the multimodal neuronavigation plan and to precisely relocate the lesions. A final intraoperative MRI scan confirmed total resection in all cases.

Table 1
Characteristics of 13 patients with supratentorial cavernomas.

Patient No	Age (years)	Gender	Location (side)	Lesion volume (cm^3)	Lesion to eloquent areas distance (mm)											Zabramski classification	Total iMRI scans
					Motor—sensory					Language			Vision				
					fMRI			DTT		fMRI		DTT	fMRI	DTT			
					H	F	L	M	S	B	W	AF	V	DB	ML		
1	10	Female	Centrum Ovale (Left)	0.20	10.8	–	–	3.6	0	–	–	8.7	–	–	–	III	3
2	32	Female	Frontal (Left)	1.83	10.4	3.8	29.3	1.4	7.8	–	–	–	–	–	–	III	1
3	19	Male	Periventricular (Right)	0.47	–	–	–	3.6	1.8	–	–	–	–	–	–	III	3
4	10	Male	Centrum Ovale (Left)	11.45	4.6	–	5.5	1.4	1.6	–	–	5.2	–	–	–	III	1
5	51	Female	Temporal (Left)	1.83	–	–	–	–	–	–	–	–	–	1.9	7.5	I	1
6	61	Male	Trigono (Left)	10.05	–	–	–	12.8	7.7	–	–	12.5	–	4.9	1.4	I	1
7	40	Female	Temporal (Right)	2.05	–	–	–	–	–	–	–	–	–	5.3	0	III	1
8	21	Male	Temporal (Right)	2.87	–	–	–	–	–	–	–	–	–	3.6	2.6	III	1
9	26	Female	Occipital (Right)	2.86	–	–	–	–	–	–	–	–	8.1	11.6	12.3	II	2
10	55	Male	Bifrontal (Left)	0.47	–	–	–	31.0	–	–	–	–	–	–	–	II	2
			(Right)	0.34	–	–	–	56	–	–	–	–	–	–	–	II	
11	53	Male	Thalamus (Right)	0.51	–	–	–	2.4	0	–	–	–	–	5.6	6.3	III	3
12	58	Female	Insular (Left)	0.97	–	–	–	3.7	5.5	–	–	4.5	–	11.4	14.5	III	1

fMRI: functional magnetic resonance imaging; DTT: functional magnetic resonance imaging; iMRI: intraoperative magnetic resonance imaging; H: hand cortex; F: foot cortex; L: lips cortex; M: corticospinal tracts; S: medial lemniscus; B: Broca's area; W: Wernick's area; AF: arcuate fasciculus; V: visual occipital cortex; DB: dorsal bundles; ML: Meyer's loop.

Neurological evaluation and clinical follow-up

Results from the neurological evaluations of all patients are shown in Table 2. Clinical follow-up was performed for a period between 4 months and 24 months. Some or all presenting signs and symptoms were improved or resolved in 4 cases, but were unchanged in 7 patients.

A simplified version of Engel's classification[23,24] was used to evaluate long-term seizure outcomes. Out of the 9 cases presenting with epilepsy, 7 patients had an Engel class Ⅰ outcome (seizure-free), 1 had a class Ⅱ (rare seizures, less than 12 per year) outcome, and 1 had a class Ⅲ (worthwhile improvement) outcome.

Illustrative case

A 32-year-old female patient presented with pharmaco-resistant epilepsy for 4 years (patient 2 in Tables 1 and 2). A preoperative MRI showed a mixed-signal lesion with a surrounding hypointense rim in the left supplementary motor area (Fig. 1A and B). The primary diagnosis was Zabramski Classification type Ⅲ cavernous malformation. The hand, foot, and lip cortices were successfully activated as indicated by BOLD-fMRI. The corticospinal tracts and medial lemniscuses were also depicted using DTI-based fiber tracking (Fig. 1C and D). The minimum distances between the lesions and the hand, foot, and lip cortices, corticospinal tracts, and the medial lemniscus were approximately 10.4 mm, 3.8 mm, 29.3 mm, 1.4 mm, and 7.8 mm, respectively. The preoperative neurological evaluation was normal.

The patient underwent intraoperative MRI, multimodal neuronavigation, and intraoperative electrophysiological monitoring-guided resection of a left supplementary motor area cavernoma (Fig. 2A and B). After dura opening, direct cortical stimulation was performed to identify the precentral gyrus. MEPs of the corresponding muscles were recorded. Intraoperative identification of the precentral gyrus, and the hand, foot and lip cortices, which were enabled by direct cortical stimulation, was consistent with the preoperative fMRI findings. After resection, intraoperative MRI confirmed the total resection of the nidus and excluded any post-resectional hemorrhagic or ischemic deficits (Fig. 2C and D). Intraoperative DTI-based fiber tracking showed that the major white matter tracts, such as the corticospinal tracts and the medial lemniscuses, were intact (Fig. 2E and F). No postoperative neurological deficits were found in this patient.

At the 8-month follow-up, the patient had an Engel class Ⅰ outcome (seizure-free). A follow-up MRI scan confirmed the total resection of the cavernoma (Fig. 3A and B). The hand, foot, and lip cortices were successfully activated in a follow-up BOLD-fMRI. The corticospinal tracts and the medial lemniscuses were also traced using follow-up DTI-based fiber tracking (Fig. 3C and D).

Table 2
13 patient's pre- and postoperative clinical assessment of supratentorial cavernomas.

Patient No	Presenting symptoms	Preoperative clinical assessment	At discharge (short-term)	Follow-up periods (months)	Postoperative clinical assessment (long-term)
1	Seizure	Right mild paresthesia	Right motor strength grade II Right severe paresthesia	18	Right motor strength grade IV+ Right mild paresthesia, seizure free
2	Seizure	Normal	Normal	8	No deficits Seizure free
3	Left hemiparesis	Left motor strength grade IV+ Left moderate paresthesia	Left motor strength grade IV+ Left moderate paresthesia	21	No deficits
4	Right hemiparesis	Right motor strength grade IV Right severe paresthesia	Right motor strength grade IV− Right severe paresthesia Slight aphasia	22	No deficits
5	Seizure	Normal	Normal	4	No deficits Seizure class III
6	Seizure	Normal	Normal	12	No deficits Seizure free
7	Seizure	Quadrantanopia	Quadrantanopia	24	Improved Seizure class II
8	Seizure	Normal	Normal	14	No deficits Seizure free
9	Seizure	Normal	Normal	20	No deficits Seizure free
10	Seizure	Normal	Normal	24	No deficits Seizure free
11	Left paresthesia	Left moderate paresthesia	Left motor strength grade IV− Left severe paresthesia	19	Left motor strength grade V Left mild paresthesia
12	Seizure	Normal	Normal	8	No deficits Seizure free

Discussion

Intraoperative MRI and multimodal neuronavigation have become promising techniques for neurosurgical interventions and in brain function research.[16,25–29] In our previous studies, we have clearly demonstrated the accuracy and validity of intraoperative MRI, DTI-based fiber tracking, and fMRI in standard neurosurgical procedures.[14,15,22,30] Here we investigated the feasibility of intraoperative MRI and multimodal neuronavigation for the treatment of supratentorial cavernomas.

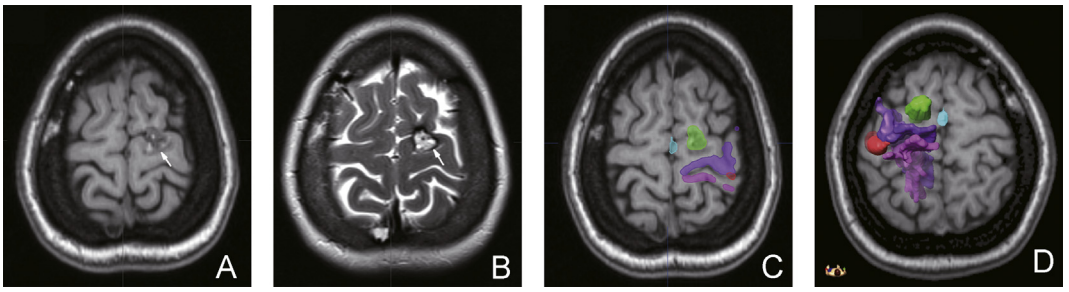

Fig. 1. A 32-year-old female patient (Patient 2 in Table 1) presented with pharmaco-resistant epilepsy. A–B. Conventional MRI showed a mixed-signal lesion (white arrow) with a surrounding hypointense rim in the left supplementary motor area. C–D. A 3D reconstructed view revealed the relationships between the lesion (green) and the hand cortex (red), corticospinal tracts (purple), medial lemniscus (pink), and foot cortex (sky blue).

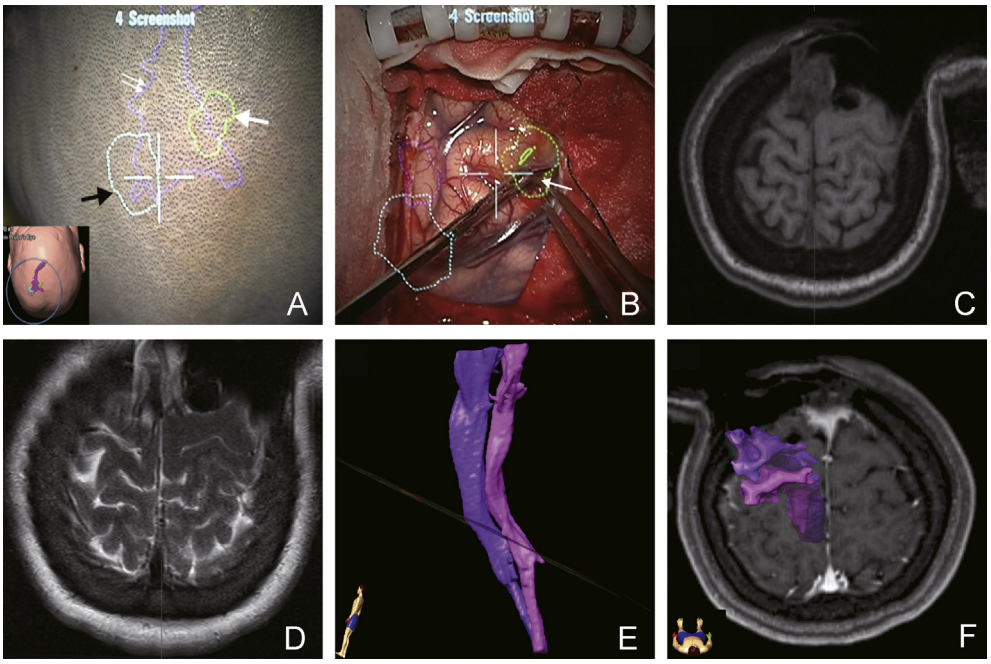

Fig. 2. A 32-year-old female patient (Patient 2 in Table 1) presented with pharmaco-resistant epilepsy. A. Intraoperatively navigated microscopic view before craniotomy. Contours of the lesion (green, white arrow), hand cortex (sky blue, black arrow) and corticospinal tracts (purple, double arrow) were projected onto the scalp and facilitated craniotomy. B. A navigated microscopic view exposed the posterior part of the lesion (white arrow, green contour). Hand cortex (sky blue contour), lip cortex (purple contour). C−D. Multimodal intraoperative MR imaging showed complete resection of the nidus. E−F. An intraoperative 3D-reconstructed view revealed that the corticospinal tracts (purple) and medial lemniscus (pink) were intact.

The preoperative determination of 3D relationships between lesions and surrounding eloquent structures enabled the use of a smaller tailored craniotomy and a corticectomy very near the lesions. Intraoperative MRI, multimodal neuronavigation, and the integral use of intraoperative electrophysiological monitoring can provide instant intraoperative quality control, be used to evaluate the extent of the resection, correct for brain shifts, and update surgical strategies when necessary.

Seizure is the most common symptom associated with supratentorial cavernomas, of which approximately 40% are medically refractory.[31−33] Surgical resection is a safe and effective treatment for minimizing the seizure burden in patients with supratentorial cavernomas.[33] Supratentorial cavernomas involving non-eloquent structures are supposed to undergo aggressive resection.[33] However, surgical treatment of symptomatic cavernomas involving critical areas remains risky.

Eleven of the 12 patients had lesions involving nearby eloquent structures (<1 cm away). One patient harbored two bilateral deep-seated lesions in the frontal lobes. Eight small cavernomas were present in the 12 patients. Ten lesions were deeply seated in subcortical areas. In this study cohort, intraoperative MRIs were performed more than once in 5 patients to update the multimodal neuronavigation plan, correct for brain shifts, and relocate the niduses. Preoperatively, the surgeons had estimated severe brain shifts in 2 cases. Although the *P* value (0.37) was not deemed statistically significant, the surgical procedures were facilitated by intraoperative MRI. All 13 cavernomas were treated by neurosurgical procedures guided by intraoperative MRI, multimodal neuronavigation, and intraoperative electrophysiological monitoring. In a patient with a lesion adjacent to the precentral gyrus, intraoperative identification of the precentral gyrus and the hand, foot, and lip cortices by direct cortical stimulation was consistent with preoperative fMRI findings, as shown in the navigated microscopic view (Fig. 1B).

Nine out of 12 patients with supratentorial cavernomas presented with seizures, four of which were refractory to anti-epilepsy drugs. In these 4 patients, 2 patients had a class Ⅰ outcome, 1 had a class Ⅱ outcome, and 1 had a class Ⅲ outcome. The other 5 patients had a class Ⅰ postoperative outcome.

The goal of supratentorial cavernoma surgery is to maximize the resection of the nidus and epileptic foci while preserving neurological function. Intraoperative

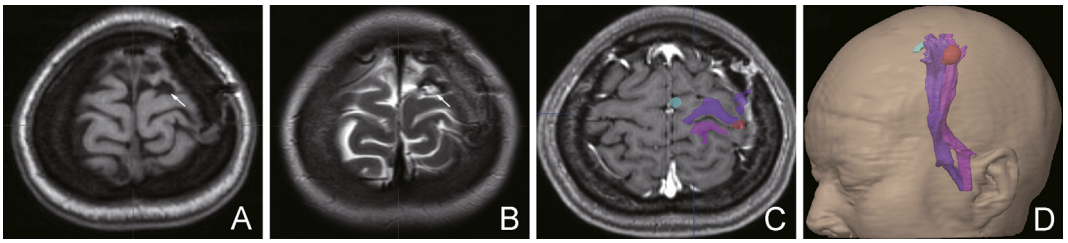

Fig. 3. A 32-year-old female patient (Patient 2 in Table 1) presented with pharmaco-resistant epilepsy. A−B. Postoperative follow-up MR imaging confirmed the total resection of lesion (white arrow). C−D. A 3D reconstructed view showed the corticospinal tracts (purple), medial lemniscus (pink), hand cortex (red) and foot cortex (sky blue).

MRI assists with intraoperative real-time visualization of the lesion remnants and the surrounding eloquent structures.

Conclusions

Our results suggest that selected small, deep-seated cavernomas involving critical areas are optimal candidates for treatment with intraoperative MRI, multimodal neuronavigation and intraoperative electrophysiological monitoring.

Conflicts of interest

The authors have no personal, financial, or institutional interest in any of the drugs, materials, or devices described in this article.

Acknowledgements

This study was supported by the National Natural Science Foundation (NCSF) of China (81271515) and The Science Technological Innovation Nursery Fund of PLA General Hospital (16KMM14).

References

1. Martin C, Alexander 3rd E, Wong T, et al. Surgical treatment of low-grade gliomas in the intraoperative magnetic resonance imager. *Neurosurg Focus*. 1998;4:e8.
2. Alexander 3rd E, Moriarty TM, Kikinis R, et al. The present and future role of intraoperative MRI in neurosurgical procedures. *Stereotact Funct Neurosurg*. 1997;68:10−17.
3. Moriarty TM, Kikinis R, Jolesz FA, et al. Magnetic resonance imaging therapy. Intraoperative MR imaging. *Neurosurg Clin N Am*. 1996;7:323−331.
4. Nimsky C, Ganslandt O, von Keller B, et al. Preliminary experience in glioma surgery with intraoperative high-field MRI. *Acta Neurochir Suppl*. 2003;88:21−29.
5. Nimsky C, Ganslandt O, Gralla J, et al. Intraoperative low-field magnetic resonance imaging in pediatric neurosurgery. *Pediatr Neurosurg*. 2003;38:83−89.
6. Fahlbusch R, Ganslandt O, Buchfelder M, et al. Intraoperative magnetic resonance imaging during transsphenoidal surgery. *J Neurosurg*. 2001;95:381−390.
7. Fahlbusch R, Ganslandt O, Nimsky C. Intraoperative imaging with open magnetic resonance imaging and neuronavigation. *Childs Nerv Syst*. 2000;16:829−831.
8. Senft C, Bink A, Heckelmann M, et al. Glioma extent of resection and ultra-low-field iMRI: interim analysis of a prospective randomized trial. *Acta Neurochir Suppl*. 2011;109:49−53.
9. Kuhnt D, Bauer MH, Becker A, et al. Intraoperative visualization of fiber tracking based reconstruction of language pathways in glioma surgery. *Neurosurgery*. 2012;70:911−919.
10. Sutherland GR, Kaibara T, Wallace C, et al. Intraoperative assessment of aneurysm clipping using magnetic resonance angiography and diffusion-weighted imaging: technical case report. *Neurosurgery*. 2002;50:893−897.
11. Gralla J, Ganslandt O, Kober H, et al. Image-guided removal of supratentorial cavernomas in critical brain areas: application of neuronavigation and intraoperative magnetic resonance imaging. *Minim Invasive Neurosurg*. 2003;46:72−77.
12. Berntsen EM, Gulati S, Solheim O, et al. Integrated pre- and intraoperative imaging in a patient with an arteriovenous malformation located in eloquent cortex. *Minim Invasive Neurosurg*. 2009;52:83−85.
13. Chang EF, Wang DD, Barkovich AJ, et al. Predictors of seizure freedom after surgery for malformations of cortical development. *Ann Neurol*. 2011;70:151−162.
14. Chen X, Xu BN, Meng X, et al. Dual-room 1.5-T intraoperative magnetic resonance imaging suite with a movable magnet: implementation and preliminary experience. *Neurosurg Rev*. 2012;35:95−109.
15. Sun GC, Chen XL, Zhao Y, et al. Intraoperative high-field magnetic resonance imaging combined with fiber tract neuronavigation-guided resection of cerebral lesions involving optic radiation. *Neurosurgery*. 2011;69:1070−1084.
16. Nimsky C, Ganslandt O, Merhof D, et al. Intraoperative visualization of the pyramidal tract by diffusion-tensor-imaging-based fiber tracking. *NeuroImage*. 2006;30:1219−1229.
17. Shewan CM, Kertesz A. Reliability and validity characteristics of the Western Aphasia Battery (WAB). *J Speech Hear Disord*. 1980;45:308−324.
18. Dyck PJ, Boes CJ, Mulder D, et al. History of standard scoring, notation, and summation of neuromuscular signs. A current survey and recommendation. *J Peripher Nerv Syst*. 2005;10:158−173.
19. Vanhoutte EK, Faber CG, van Nes SI, et al. Modifying the Medical Research Council grading system through Rasch analyses. *Brain*. 2012;135:1639−1649.

20. Zabramski JM, Wascher TM, Spetzler RF, et al. The natural history of familial cavernous malformations: results of an ongoing study. *J Neurosurg*. 1994;80:422−432.
21. Kivelev J, Niemela M, Kivisaari R, et al. Long-term outcome of patients with multiple cerebral cavernous malformations. *Neurosurgery*. 2009;65:450−455.
22. Sun GC, Chen XL, Zhao Y, et al. Intraoperative MRI with integrated functional neuronavigation-guided resection of supratentorial cavernous malformations in eloquent brain areas. *J Clin Neurosci*. 2011;18:1350−1354.
23. Moran NF, Fish DR, Kitchen N, et al. Supratentorial cavernous haemangiomas and epilepsy: a review of the literature and case series. *J Neurol Neurosurg Psychiatry*. 1999;66:561−568.
24. Wheeler M, De Herdt V, Vonck K, et al. Efficacy of vagus nerve stimulation for refractory epilepsy among patient subgroups: a re-analysis using the Engel classification. *Seizure*. 2011;20:331−335.
25. Chicoine MR, Lim CC, Evans JA, et al. Implementation and preliminary clinical experience with the use of ceiling mounted mobile high field intraoperative magnetic resonance imaging between two operating rooms. *Acta Neurochir Suppl*. 2011;109:97−102.
26. Hall WA, Kim P, Truwit CL. Functional magnetic resonance imaging-guided brain tumor resection. *Top Magn Reson Imaging*. 2009;19:205−212.
27. Kuhnt D, Becker A, Ganslandt O, et al. Correlation of the extent of tumor volume resection and patient survival in surgery of glioblastoma multiforme with high-field intraoperative MRI guidance. *Neuro Oncol*. 2011;13:1339−1348.
28. Kuhnt D, Ganslandt O, Schlaffer SM, et al. Quantification of glioma removal by intraoperative high-field magnetic resonance imaging: an update. *Neurosurgery*. 2011;69:852−862.
29. Nimsky C, Kuhnt D, Ganslandt O, et al. Multimodal navigation integrated with imaging. *Acta Neurochir Suppl*. 2011;109:207−214.
30. Zhao Y, Chen X, Wang F, et al. Integration of diffusion tensor-based arcuate fasciculus fibre navigation and intraoperative MRI into glioma surgery. *J Clin Neurosci*. 2012;19:255−261.
31. Ryvlin P, Mauguiere F, Sindou M, et al. Interictal cerebral metabolism and epilepsy in cavernous angiomas. *Brain*. 1995;118:677−687.
32. Englot DJ, Han SJ, Lawton MT, et al. Predictors of seizure freedom in the surgical treatment of supratentorial cavernous malformations. *J Neurosurg*. 2011;115:1169−1174.
33. Chang EF, Gabriel RA, Potts MB, et al. Seizure characteristics and control after microsurgical resection of supratentorial cerebral cavernous malformations. *Neurosurgery*. 2009;65:31−37.

Edited by Jing-Ling Bao